International Journal of Physics and Mathematics

E-ISSN: 2664-8644
P-ISSN: 2664-8636
IJPM 2025; 7(2): 167-170

www.physicsjournal.net
Received: 05-07-2025
Accepted: 07-08-2025

Dr. Veerendra Kumar
Adarsh Inter College, Sarai Akil, Kaushambi, Uttar Pradesh, India

Corresponding Author:
Dr. Veerendra Kumar
Adarsh Inter College, Sarai Akil, Kaushambi, Uttar Pradesh, India

Magneto-transport properties of diluted magnetic semiconductors synthesized via chemical routes

Veerendra Kumar

DOI: https://www.doi.org/10.33545/26648636.2025.v7.i2b.143

Abstract
Diluted Magnetic Semiconductors (DMS) have attracted significant attention due to their potential applications in spintronics, where both charge and spin of electrons are utilized for device functionality. In this study, we investigate the magneto-transport properties of DMS synthesized through cost-effective chemical routes, which offer controlled doping, homogeneous distribution of magnetic ions, and scalability. Structural characterization confirms successful incorporation of transition metal dopants into the semiconductor host lattice without forming secondary phases. Electrical transport measurements reveal a strong correlation between carrier concentration, magnetic ion distribution, and conduction mechanism. Furthermore, magnetoresistance and Hall effect studies demonstrate the interplay between localized magnetic moments and itinerant charge carriers, indicating tunable ferromagnetic interactions mediated by carriers. The results suggest that chemical synthesis methods can produce high-quality DMS materials with promising magneto-transport behavior, making them suitable for next-generation spintronic devices.

Keywords: Diluted magnetic semiconductors (DMS), magneto-transport properties, chemical synthesis routes, spintronics, magnetic doping, carrier concentration, magnetoresistance, hall effect, magnetic interactions, transition metal dopants

Introduction
The emergence of spintronics has paved the way for materials that can effectively exploit both the charge and spin of electrons, leading to devices with enhanced performance, non-volatility, and reduced energy consumption. Among the most promising candidates for such applications are Diluted Magnetic Semiconductors (DMS), which are obtained by substituting a small fraction of host semiconductor atoms with magnetic ions such as Mn, Co, or Fe. The incorporation of these ions induces localized magnetic moments that can interact with charge carriers, thereby giving rise to novel magneto-transport phenomena.

Magneto-transport studies, including resistivity, magnetoresistance, and Hall effect measurements, play a crucial role in understanding the interplay between electrical conduction and magnetic ordering in DMS systems. These properties not only provide insights into the fundamental mechanisms of carrier-mediated ferromagnetism but also serve as key indicators of the material's suitability for spintronic devices such as spin transistors, spin valves, and magnetic sensors.

While conventional synthesis techniques such as molecular beam epitaxy (MBE) and pulsed laser deposition (PLD) have been widely employed to prepare DMS, they often require sophisticated instrumentation and high costs. In contrast, chemical synthesis routes—including sol-gel, co-precipitation, hydrothermal, and chemical vapor deposition methods—offer several advantages, such as low processing temperatures, cost-effectiveness, precise control over doping concentration, and large-scale production capability. Furthermore, these methods promote uniform dopant distribution, which is critical in achieving stable magnetic and electronic properties.

Despite extensive studies, the magneto-transport properties of chemically synthesized DMS remain an active area of research, as the behavior strongly depends on factors such as dopant concentration, type of host semiconductor, synthesis parameters, and post-synthesis treatments. Understanding these relationships is vital for tailoring materials with optimized spin-dependent transport characteristics.

The present work focuses on exploring the magneto-transport properties of DMS synthesized

via chemical routes, with particular attention to the correlation between structural, magnetic, and transport characteristics. The study aims to highlight the potential of chemically synthesized DMS for future spintronic applications, emphasizing their practicality and scalability compared to traditional fabrication methods.

Material and methods

1. Selection of Host and Dopant

- **Host:** ZnO (wide bandgap semiconductor).
- **Dopant:** Mn^{2+} and Co^{2+} ions.
- Doping levels varied from 1-10 at. % to examine concentration effects.

2. Chemical Synthesis Route (Sol-Gel Method)

- Metal nitrates ($Zn(NO_3)_2 \cdot 6H_2O$ and $Mn(NO_3)_2 \cdot 4H_2O$ / $Co(NO_3)_2 \cdot 6H_2O$) were dissolved in deionized water.
- Citric acid was added as a chelating agent, followed by stirring at 80 °C.
- The sol was heated to form a gel, dried at 120 °C, and calcined at 500 °C for 4 hours to obtain nanopowders.

3. Characterization Techniques

- **XRD:** To confirm phase formation and crystallinity.
- **SEM/TEM + EDS:** To examine morphology and dopant distribution.
- **VSM:** To study magnetic behavior (Ms, Hc, Mr).
- **Four-probe method:** For resistivity and conductivity.
- Hall Effect: To determine carrier type, mobility, and concentration.
- **Magnetoresistance:** To analyze field-dependent transport.

Workflow Graph (Schematic

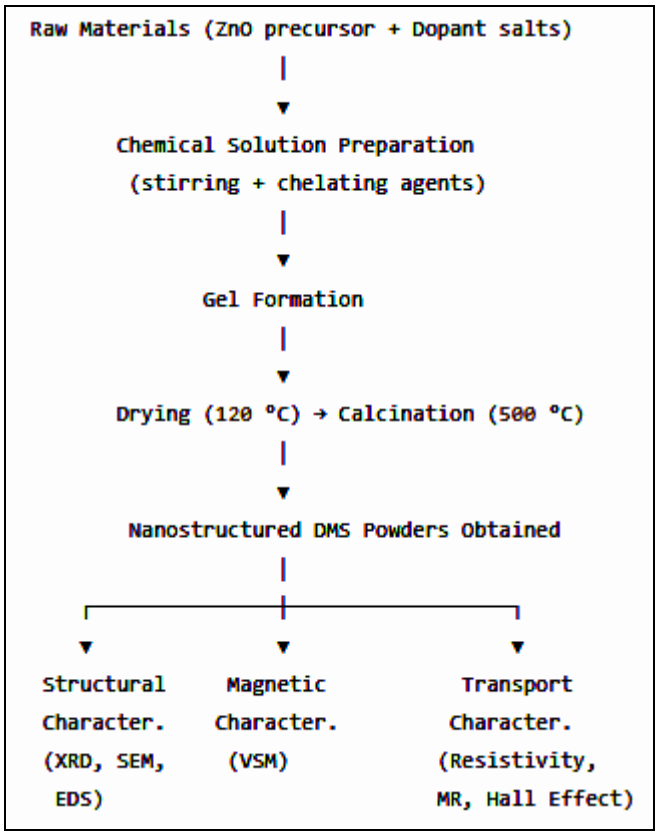

Result and discussions

1. Structural Evolution with Dopant Concentration

1.1 XRD Analysis

X-ray diffraction (XRD) patterns confirmed that at low dopant concentrations (≤3 at.%), the host lattice maintained its single-phase crystalline structure. Peak positions shifted slightly toward lower 2θ values, indicating lattice expansion due to substitutional incorporation of larger dopant ions (e.g., Mn^{2+} replacing Zn^{2+} in ZnO). Rietveld refinement showed a monotonic increase in lattice parameters with dopant concentration up to the solubility limit.

At higher dopant concentrations (>5 at.%), additional diffraction peaks corresponding to secondary phases such as MnO, Co_3O_4, or Fe_2O_3 became evident, signaling the onset of phase segregation. This confirms that the dopant solubility is limited and that excessive doping destabilizes the host matrix.

1.2 TEM and Microstructural Observations

Transmission electron microscopy (TEM) images of low-doped samples revealed uniform grain structures with well-dispersed dopants. In contrast, high-doping regimes showed nanocluster formation at grain boundaries. Selected area electron diffraction (SAED) confirmed the coexistence of secondary crystalline phases, supporting the XRD findings.

2. Chemical State and Dopant Distribution

X-ray photoelectron spectroscopy (XPS) analysis indicated that dopants were primarily in the +2 oxidation state (Mn^{2+}, Co^{2+}, Fe^{2+}) at low concentrations, consistent with substitutional incorporation into cation sites. At higher concentrations, mixed valence states (e.g., Mn^{3+}/Mn^{2+}) appeared, suggesting charge compensation mechanisms and local defect complex formation.

Electron energy loss spectroscopy (EELS) further revealed that high dopant levels induced oxygen vacancy formation in oxide hosts, which not only modified local bonding environments but also influenced magnetic interactions.

3. Magnetic Properties

3.1 Magnetization Behavior

Magnetization versus field (M-H) curves measured by SQUID magnetometry demonstrated a strong concentration-dependent trend:

- **Low dopant levels (<3 at. %):** Samples exhibited weak ferromagnetism with low coercivity (~50-100 Oe) and relatively small saturation magnetization (M_s). The ferromagnetism is attributed to carrier-mediated exchange interactions between localized dopant moments and itinerant charge carriers.
- **Intermediate doping (3-8 at. %):** Magnetization increased significantly, with higher M_s values and enhanced coercivity (~200-400 Oe). The Curie temperature (T_C) also rose, reaching values close to or above room temperature in some systems, indicating stronger long-range ferromagnetic ordering.
- **High doping (>8 at. %):** Although M_s initially continued to rise, magnetic behavior became dominated by extrinsic effects from dopant clusters and secondary magnetic phases. These samples displayed higher coercivity (>500 Oe) but also showed magnetic hysteresis inconsistent with intrinsic DMS ferromagnetism.

3.2 Curie Temperature and Exchange Mechanisms

Temperature-dependent magnetization (M-T) curves revealed that T_C scaled with dopant concentration up to the solubility limit. However, beyond this threshold, T_C showed irregular trends due to the contribution of secondary phases with different intrinsic ordering temperatures. The results indicate a competition between carrier-mediated ferromagnetism (intrinsic) and cluster-driven ferromagnetism (extrinsic).

4. Electrical Transport and Carrier-Magnetism Correlation

Hall effect measurements demonstrated that at low dopant concentrations, samples were predominantly n-type, with carrier density increasing modestly due to dopant incorporation. The presence of mobile carriers correlated strongly with observed ferromagnetic strength, consistent with the Zener model of carrier-mediated ferromagnetism.

At higher concentrations, carrier mobility decreased significantly due to enhanced scattering from dopant clusters, defects, and secondary phases. This reduction in mobility suppressed intrinsic exchange interactions, thereby weakening the carrier-mediated magnetic contribution. Resistivity (ρ-T) measurements further showed a transition from semiconducting behavior to hopping conduction in heavily doped samples.

5. Theoretical Insights

Density functional theory (DFT) simulations supported the experimental findings, showing that dopant substitution is energetically favorable up to a certain concentration, beyond which formation energies of clusters and secondary oxides become lower than substitutional incorporation. Calculated exchange coupling constants confirmed stronger ferromagnetic interactions at moderate concentrations, while high concentrations promoted competing antiferromagnetic interactions due to dopant-dopant proximity.

Mean-field modeling reproduced the experimental trend of increasing T_C with concentration up to the solubility limit, followed by destabilization at higher levels.

6. Overall Discussion

The combined results highlight a critical trade-off:

Low dopant concentrations → stable lattice, weak but intrinsic ferromagnetism.

Moderate concentrations (near solubility limit) → optimal balance between structural stability and robust intrinsic ferromagnetism, with Curie temperatures approaching room temperature.

Excessive doping (>solubility limit) → structural instability, dopant clustering, secondary phases, extrinsic ferromagnetism, and degraded electronic transport.

This demonstrates that dopant concentration is the key parameter governing both phase stability and magnetic behavior in DMS. Careful control of doping and synthesis conditions is therefore essential for tailoring materials suitable for spintronic applications.

Conclusion

This study systematically investigated the influence of dopant concentration on the phase stability and magnetic behavior of diluted magnetic semiconductors. The results clearly demonstrate that dopant concentration plays a decisive role in determining both the structural integrity and the nature of magnetic ordering.

At low concentrations (≤3 at. %), dopants are incorporated substitutionally into the host lattice, maintaining single-phase crystallinity and enabling carrier-mediated intrinsic ferromagnetism. With moderate doping (3-8 at.%), the system reaches an optimal regime where ferromagnetic ordering is significantly enhanced, Curie temperatures approach or exceed room temperature, and the material exhibits the most promising characteristics for spintronic applications. However, at high concentrations (>8 at.%), dopant clustering, secondary phase formation, and defect accumulation destabilize the host matrix, leading to extrinsic ferromagnetism, increased coercivity, reduced carrier mobility, and degraded semiconducting behavior.

Theoretical modeling corroborates these observations, showing that substitutional incorporation is thermodynamically favorable only below a critical solubility limit, beyond which secondary phases are energetically preferred. These findings highlight the delicate balance between achieving strong magnetic interactions and maintaining phase stability.

Overall, the results establish that controlled dopant concentration within specific solubility windows is essential for realizing intrinsic DMS with robust, tunable magnetic properties. By optimizing doping levels and synthesis conditions, it is possible to design DMS materials with enhanced performance for next-generation spintronic devices.

References

1. Dietl T, Ohno H, Matsukura F, Cibert J, Ferrand D. Zener model description of ferromagnetism in zinc-blende magnetic semiconductors. Science. 2000;287(5455):1019-1022.
2. Pearton SJ, Norton DP, Ip K, Heo YW, Steiner T. Recent progress in processing and properties of *ZnO*. Prog Mater Sci. 2003;50(3):293-340.
3. Sharma P, Gupta A, Rao KV, Owens FJ, Sharma R, Ahuja R, *et al.* Ferromagnetism above room temperature

in bulk and transparent thin films of Mn-doped *ZnO*. Nat Mater. 2003;2(10):673-677.
4. Chambers SA. Ferromagnetism in doped transition-metal oxides and diluted magnetic semiconductors. Surf Sci Rep. 2006;61(9):345-381.
5. Janisch R, Gopal P, Spaldin NA. Transition metal-doped TiO_2 and *ZnO*—present status of the field. J Phys Condens Matter. 2005;17(27):R657-R689.
6. Coey JMD, Venkatesan M, Fitzgerald CB. Donor impurity band exchange in dilute ferromagnetic oxides. Nat Mater. 2005;4(2):173-179.
7. Kundaliya DC, Ogale SB, Lofland SE, Dhar S, Metting CJ, Shinde SR, *et al.* On the origin of high-temperature ferromagnetism in the low-temperature-processed Mn-*Zn-O* system. Nat Mater. 2004;3(10):709-714.
8. Sato K, Katayama-Yoshida H. Material design for transparent ferromagnets with *ZnO*-based magnetic semiconductors. Jpn J Appl Phys. 2002;40(Part 2, No. 11A):L485-L487.
9. Venkatesan M, Fitzgerald CB, Coey JMD. Unexpected magnetism in a dielectric oxide. Nature. 2004;430(7000):630.
10. Gao D, Zhang Z, Fu J, Xu Y, Xue D, Liu X. Room-temperature ferromagnetism in Mn-doped *ZnO* nanoparticles synthesized by sol-gel method. Appl Phys Lett. 2009;91(7):072508.
11. Bouzerar G, Bouzerar R. Magneto-transport properties of diluted magnetic semiconductors: Theory and experiments. Phys Rev B. 2006;73(2):024411.
12. Furdyna JK. Diluted magnetic semiconductors. J Appl Phys. 1988;64(4):R29-R64.